MODELING, IDENTIFICATION AND CONTROL, 1995, VOL. 16, NO. 4, 233–241
doi:10.4173/mic.1995.4.4

Mechanical analysis of high precision manipulator

O. J. ELLE†, K. JOHNSEN† and T. K. LIEN†

Keywords: *Manipulator, mechanism analysis, deflection, dynamics, resonance frequency.*

It is of great importance that high precision manipulators are well designed from a mechanical point of view. A thorough analysis of all mechanical aspects concerning an accurate manipulator will make a good basis for further design. This paper presents a new approach to mechanical analysis of high-precision manipulators. A typical six axis anthropomorphic manipulator configuration is chosen as a model for the analysis. The paper is divided into two main parts; static deformation analysis and dynamic analysis. The static deformation analysis consists of three sub-parts; link deformation, joint deformation and total mechanical deformation. A simple fixed beam deformation model is used to simulate every link. Both specific gravity and a load attached at the end of the beam is considered. By varying material, outer dimensions and wall thickness it is possible to determine optimal values. Looking at the whole structure with an attacking force at the end, it is possible to select appropriate motor/transmission combinations. Each combination represents compliance and combined with the arm compliance the total deformation can be found. The result shows that deformation due to compliance in the joints represents 97% of the total. Based on the result of the previous section, the dynamic model can be simplified significantly. The arm elements are supposed to be rigid and all the compliances are due to the joint deformation. This gives a coupled mass/spring system to be analysed. The resonance frequencies of the system are found through theoretical analysis and through simulation in a Finite Element based program for Dynamic analysis of Elastic Mechanisms (FEDEM) (Sintef Production Engineering 1993).

1. Introduction

Stiffness is one of the most important general criteria of machine design. This is especially true for manipulators. The problem of stiffness enhancement is especially important since conventional techniques, such as 'beefing up' cross-sections or using high-modulus conventional materials, are in many cases not acceptable either because they are counter-productive and/or not cost effective. In many instances, both the external and internal dimensions of the links are limited by design and/or application constraints.

'Effective stiffness' is a frequently used phrase. This definition means a numerical expression of the response of the structure at a certain important point to performance-induced forces. Such a response (i.e., effective stiffness and compliance) is a result of four basic factors (Rivin 1988):

(1) Structural deformations of load-transmitting components which are idealized

Received 29 March 1995.
† Department of Production and Quality Engineering, Norwegian Institute of Technology, University of Trondheim, N-7034 Trondheim, Norway.

for computational purposes as beams, rods, plates, shells, etc., also with idealized loading and support conditions.

(2) Contact deformations between parts contacting along nominally small contact surfaces (e.g., balls, rollers, etc.), nominally large but actually small contact surfaces (e.g., not perfectly machined flat surfaces.

(3) Deformations in the energy-transforming devices (motors and actuators) caused by compressibility of a working medium in hydraulic and pneumatic systems, deformations of an electromagnetic field in electric motors, etc.

(4) Modifications of numerical stiffness values caused by kinematic transformations between the area in which the deformations originate and the point for which the effective stiffness is analysed.

The work that is presented in this paper was specially focused on underwater robotics. Some of the selections and conclusions are thus affected by that.

2. Static deformation analysis

The basic static force and deformation formulae are found in Irgens textbook (Irgens 1985a).

2.1. *Link deformation*

Robotic links have to comply with several constraints. Some of the constraints are as follows (Rivin 1988):

- The links should have an internal hollow area to provide conduits for electric power and communication cables, hoses, power-transmitting components, control pods, etc.
- At the same time, their external dimensions are limited in order to reduce waste of the usable workspace.
- Links have to be as light as possible to reduce inertia forces and allow for the largest payload per given size of motors and actuators.
- For a given weight, links have to possess the highest possible bending (and torsional) stiffness.

Figure 1 shows the deflection model of a simple beam. A more thorough beam analysis with different profiles and strutting is found in Opitz (1970). A vertical force F is applied at the end of a beam. The beam is of length L, height h, width b, wall thickness t, elasticity module E and cross-sectional moment of inertia I. It is horizontal and fixed in one end. The weight of the beam W, gives a distributed load $q = W*9{,}81/L$. A torque T, is attached at the end caused by moment from the next arm element. Simple calculations show that bending and/or torsional compliance is stiffness-critical for the robot structure (Rivin 1988). The vertical deflection δ_F, at the end of the beam caused by the force F, is given by

$$\delta_F = \frac{FL^3}{3EI} \tag{1}$$

Equation 2 gives the vertical deflection δ_q, at the end of the beam caused by the distributed weight of the beam.

$$\delta_q = \frac{qL^4}{8EI} \tag{2}$$

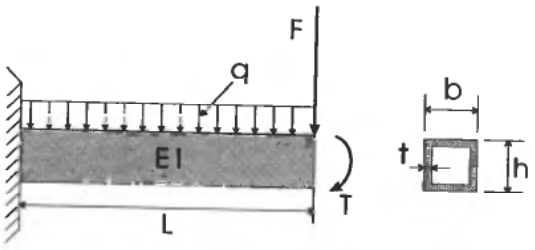

Figure 1. The deflection model.

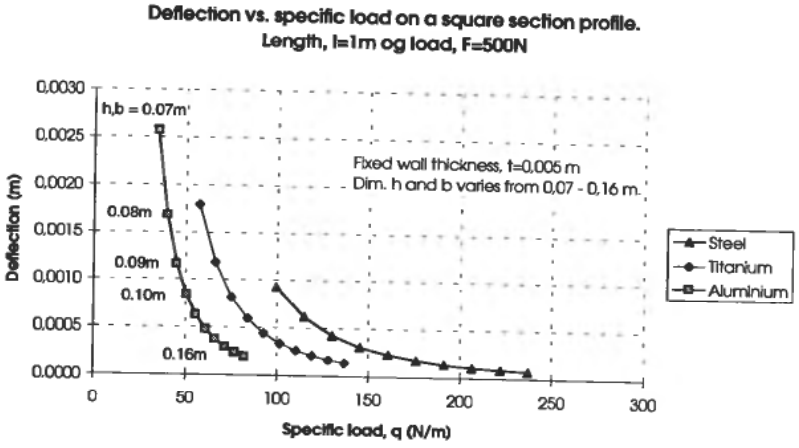

Figure 2. Deflection of the beam model with metals.

The vertical deflection δ_T, caused by the torque attacked at the end of the beam is given by

$$\delta_T = \frac{TL^2}{2EI} \tag{3}$$

The total deflection δ_{Tot}, at the end of the beam is then calculated by

$$\begin{aligned}\delta_{\text{Tot}} &= \delta_F + \delta_q + \delta_T \\ &= \frac{L^2}{EI}\left(\frac{FL}{3} + \frac{qL^2}{8} + \frac{T}{2}\right)\end{aligned} \tag{4}$$

where the cross-sectional moment of inertia I, for quadratic profiles is calculated by

$$I = \tfrac{1}{12}(bh^3 - (b-2t)(h-2t)^3) \tag{5}$$

and specific gravity q, is calculated by

$$\begin{aligned}q &= \frac{mg}{L} \\ &= \frac{\rho V g}{L} \\ &= (bh - (b-2t)(h-2t))\rho g\end{aligned} \tag{6}$$

where g is the gravitational acceleration, ρ is the material density and V is the material

volume. The torque T, results from the weight of arm elements with a distance from the beam elements further out. The deflection analysis of the beam will not include the torque influence from other elements. This will not affect the qualitative result of the analysis. The numerical values of the analysis will not be precise. The analysis is just meant to give an impression of the relative influence of changing the cross-sectional dimensions or material of the beam.

Figure 2 shows the deflection of the beam is reduced when the outer dimensions are increased. Each bullet represents the same quadratic dimension from 7–16 cm for each material selected. Observe that the difference in deflection is significant for the smaller dimensions and that it is decreasing until approximately the same deflection appears with the largest dimensions. The wall thickness and load remain constant during the dimension alteration.

The lighter material shows much higher increase in stiffness/specific weight ratio than the more heavy steel material. Aluminium showed the best property in this case. Other selection criteria, like corrosion resistance and price, have to be considered to choose between the different materials.

Figure 3 shows that changing the outer dimensions on profiles gives more stiffness per weight unit than changing the wall thickness. This is a well-known statement, but is worth mentioning. More exotic materials, like polymer composites with boron or kevlar fibres and metal composites with carbide particles, show good characteristics. Two disadvantages are the price and the problem of joining elements.

Figure 4 shows the deflection characteristic versus specific gravity of some composite materials. The best metal from Fig. 2, aluminium, is shown in comparison. As can be seen from Fig. 4, taking 0·2 mm deflection as a reference, the different materials shows different dimensions and specific gravity. The choice of material depends on which criteria to emphasise, i.e. cost, specific gravity, dimensions, stiffness etc.

2.2. *Joint deformation*

The method used in this section is based on lecture notes from Lien (Lien 1992). When the manipulator structure and arm material are selected, it is important to do some static and dynamic analysis to ensure good performance of the robot.

Figure 5 shows the arm in worst position, referred to as minimum deflection of the structure. In this position both joints 2, 3 and 4 together with link 1 and 2 contribute to the total deflection in the direction of the load. Both material selection in link 1 and 2, length of the arm elements and selection of servo/transmission systems influence this total deflection. The servo/transmission part contributes with both weight and stiffness properties. The selection of motor/transmission system on each joint of an open chain manipulator arm, has to be taken from the outer most joint and inwards to the base. The load is supposed to have a centre of gravity 5 cm from the rotation axis of joint 6 to make a realistic dimensioning torque to joint 6. This is after all not the most critical part of the structure. When maximum torque is established to the sixth joint, a proper reduction ratio is selected based on velocity criteria, necessary torque and available servo motors. With this reduction ratio a motor is selected to satisfy the new torque and velocity requirements. The weight of the selected servo/transmission combination contributes jointly with the external load to the total torque needed in joint 5. The above mentioned procedure is repeated and repeated until joint 1 is established with a motor and a reduction gear.

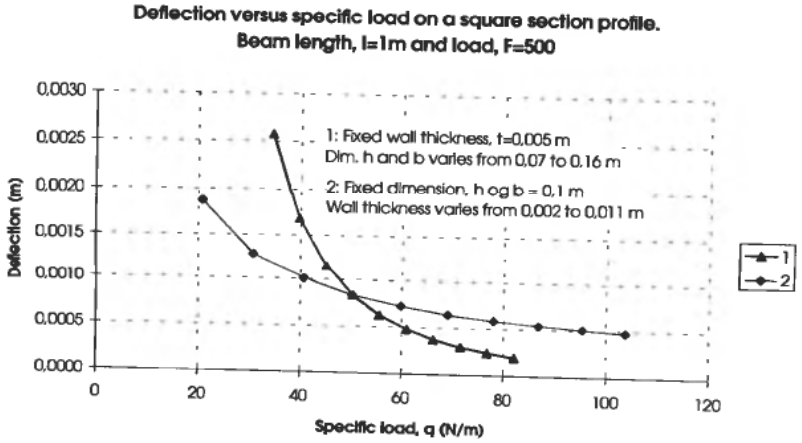

Figure 3. Different beam dimensions for aluminium and their effect on stiffness/weight ratio.

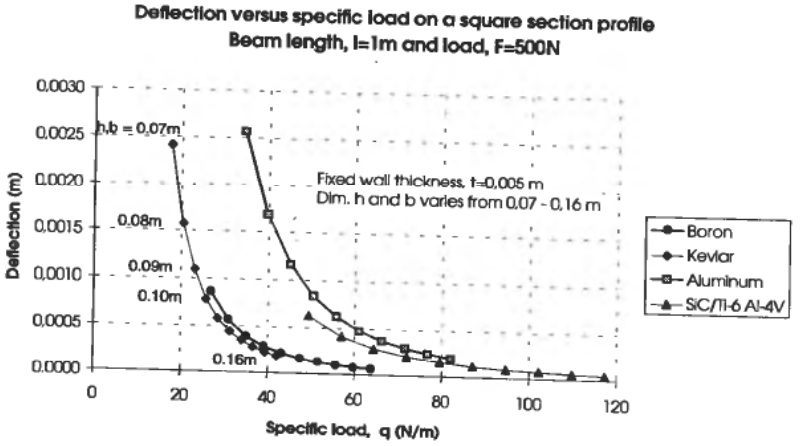

Figure 4. Deflection of the beam model with composites compared to the best metal, aluminium.

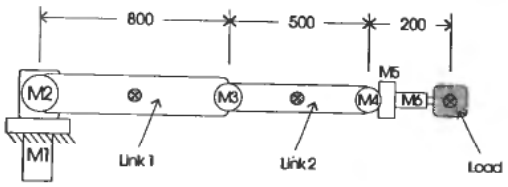

Figure 5. The anthropomorphic manipulator in worst position.

Equation 7 shows how the required motor torque T_j, is calculated for each joint starting with joint 6. The torque contribution from the links is just included where needed. Link 2 contributes to joint 3 and both link 1 and link 2 to joint 2.

$$T_j = \sum_{i=j}^{6} T_{i+1} + T_{\text{load}} + T_{\text{link}} \tag{7}$$

To ensure that the joint selection can handle supplementary dynamic peak loads, some

calculations have to be done. Assuming that the load is given an acceleration from 0–1 m/s in $t_a = 0{\cdot}20$ s. This acceleration of 5 m/s^2 gives an additional torque load of approximately one half of the static torque at the joint ($5/g = 5/9{\cdot}81 \approx 1/2$), Eqn. 8.

$$T_{\text{lin}} \approx \frac{T_j}{2} \tag{8}$$

In addition to this linear acceleration part, the joint motor has to overcome the total moment of inertia of the motor and transmission. We assume that the motor and transmission in joint (j) have moment of inertia given by:

$$J_j = J_{\text{mot}} + J_{\text{trans}} \tag{9}$$

The angular acceleration of the joint, $\ddot{\theta}_j$, is given by

$$\ddot{\theta}_j = \frac{2\pi n_j}{60}\frac{1}{t_a} \tag{10}$$

where n_j is the motor velocity given in rpm and t_a is the time for velocity increase. The additional torque from moments of inertia is given by

$$T_{\text{rot}} = J_j\ddot{\theta}_j \tag{11}$$

The total peak torque $T_{j,\text{tot}}$, is given by

$$T_{j,\text{tot}} = T_j + T_{\text{lin}} + T_{\text{rot}} \tag{12}$$

2.3. *Total structure deformation*

When the torque appearance in every joint is established, the total deflection in the structure caused by joint and beam compliance has to be found. The total deflection of the arm elements, beam 1 and beam 2, are calculated by Eqn. 4. L is the existing arm element length, q is the load caused by the weight of the element, F is the point load at the end of the beam caused by motor and gear at this point and T is the torque at the end of the beam caused by the influence of all other weights outwards to the end of the manipulator. The linear deflections of the arm, caused by rotational compliance in the joints, $\delta_{\psi j}$, are given by

$$\delta_{\psi j} = \sin(\psi_j)L_{\text{tot}} \tag{13}$$

where

$$\psi_j = \frac{T_j}{K_j}$$

In this equation ψ_j is the rotational deflection in joint j, T_j is torque in joint j, K_j is stiffness in joint j and L_{tot} is the total length from the current joint to the end of the manipulator arm. The manipulator has to stay in worst configuration (see Fig. 5) to find the total deflection of the arm. In this orientation the total linear deflection from the joints is given by

$$\delta_{\psi\,\text{tot}} = \delta_{\psi 2} + \delta_{\psi 3} + \delta_{\psi 4} \tag{14}$$

The arm element deflection of link 1 and 2 is summed and the total deflection at the end of the arm is given by

$$\delta_{\text{tot}} = \delta_{\psi\text{tot}} + \delta_1 + \delta_2 \tag{15}$$

Link	h, b [m]	t [m]	l [m]	Material
1	0·16	0·01	0·8	Steel
2	0·12	0·01	0·5	Steel

Joint	Motor	m [kg]	Gear	m [kg]	Stiffness [10^3 Nm/rad]
1	VOAC F11-10	7·5	HFUC 58	4·7	607
2	VOAC F11-10	7·5	HFUC 58	4·7	607
3	VOAC F11-5	5·0	HFUC 50	3·2	405
4	Char-Lynn 'J-Series'	2·0	HFUC 32	0·9	108
5	Char-Lynn 'J-Series	2·0	HFUC 32	0·9	108
6	Char-Lynn 'J-Series'	2·0	HFUC 20	0·98	17·5
Load	5 [kg]				

Table 1. Test data for manipulator model.

2.4. *Results and discussion*

By selecting arm links of steel, high performance harmonic drive gears and hydraulic motors (Table 1, Fig. 5), simulation has shown that the total deflection at the end of the arm is 1·39 mm. Of this only 0·03 mm was caused by deflection in the arm links.

It is interesting to observe that the compliance from the link elements is less than 3% of the total deflection. From this one can conclude that most energy should be concentrated on reducing joint compliance. Here only transmission compliance is referred, but also compliance in the motor/transmission and transmission/arm-element connection on the shafts are important to consider (Rivin 1988). To make the total manipulator system more accurate, one solution might be to measure the angular deflection of each joint from outside, and actively compensate for this in the control system. It would also be possible to measure the momentum applied by each motor and then compensate for the joint deformation based on a model of the joint.

3. Dynamic analysis

The basic dynamic formulae are found in Irgens text-book (Irgens 1985b). Based on the result of the previous chapter, the dynamic model can be simplified significantly. The arm elements are supposed to be rigid and all the compliances are due to the joint deformation. This gives a coupled mass/spring system to be analysed (see Fig. 6).

3.1. *Dynamic model*

Use of the general principles—the balance of linear momentum ($F = m^* a_c$) and the balance of angular momentum ($T_p = dL_p/dt$)—on each of the three separated links resulted in a set of equations of movement for the mechanism. In this deduction we

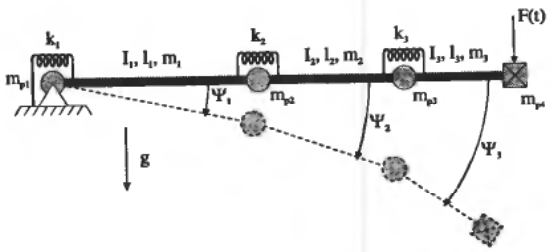

Figure 6. Sketch of the dynamic model.

assume small deflection angles. Organized in matrix form these equations result in Eqn. 16.

$$\mathbf{M}\begin{bmatrix}\ddot{\psi}_1\\ \ddot{\psi}_2\\ \ddot{\psi}_3\end{bmatrix}+\mathbf{K}\begin{bmatrix}\psi_1\\ \psi_2\\ \psi_3\end{bmatrix}=\begin{bmatrix}l_2\\ l_2\\ l_3\end{bmatrix}\mathbf{F}(t) \tag{16}$$

In this equation both the mass matrix $\boldsymbol{M}$, and the stiffness matrix $\boldsymbol{K}$, is 3×3 matrices. This is a set of three second order linear differential equations. To find the resonance frequencies, which was the main goal for this operation, we assumed a solution on the form

$$\psi_i = \psi_{io}\cos(\omega t - \phi) \tag{17}$$

By calculating the determinant of the resulting coefficient matrix and setting this equation to zero, the resonance frequencies can be found. The analysed system results in an equation of degree six, which gives three real and positive roots which are associated with the resonance frequencies of the system.

3.2. *Results and discussion*

Based on the model data from Table 1, the math program MAPLE V (Char *et al.*, 1988) was used to find the resonance frequencies of the system

$$\omega_1 = 14{\cdot}8\,\text{Hz}$$
$$\omega_2 = 74{\cdot}6\,\text{Hz}$$
$$\omega_3 = 159{\cdot}6\,\text{Hz}$$

With the lowest resonance frequency about 15 Hz, the bandwidth of the servo control system must be below this frequency. On the other hand, the control system must be fast enough to fulfil the performance criteria. One way to increase the resonance frequency of the system is to use stiffer drives. Joint one is intuitively the one that influences the lowest resonance frequency the most. Assuming a one dimensional mass/spring system doubling the resonance frequency would require four times the stiffness (Eqn. 18)

$$\omega_0 = \sqrt{\frac{k}{m}} \tag{18}$$

The robot was also modeled in a Finite Element based program for Dynamic analysis of Elastic Mechanisms, called FEDEM (SINTEF Production Engineering 1993). This analysis gave the same results as the classical dynamic calculation of a coupled

mass/spring-system within a 1·5% margin. A model of the mechanism in FEDEM gives much more flexibility in changing parameters and observation of the influence of these changes. With a spring stiffness of four times the previous modeled one, this analysis showed a rise in resonance frequency of about 70%. This is because it is a coupled system and some frequency rise was also observed in the other joints.

4. Conclusions

Based on underwater requirements we chose an anthropomorphic arm configuration to be analysed (Fig. 5). Three metal materials (steel, titanium and aluminium) and three different composite materials (boron, kevlar and siliconcarbide) were examined to try to find the best selection for our purpose. Among the metals, aluminium showed the best stiffness/specific-weight ratio under given conditions (Fig. 2). The deflection approximated the same value for the different materials with increasing dimensions—h, b. The composite materials showed even better properties (see Fig. 4) but they are expensive and joining of elements is difficult.

By selecting arm links of steel, high performance harmonic drive gears and hydraulic motors (Table 1, Fig. 5), simulation has shown that the total deflection at the end of the arm is 1·39 mm. Of this only 0·03 mm was caused by deflection in the arm links. This is less than 3% of the total deflection and it shows that the main effort should be put into reducing joint compliance. The resonance frequencies of the manipulator system are of great importance. It is very important that the joint feedback control system operates below these frequencies to avoid instabilities. The lowest resonance frequency in the modeled system was about 15 Hz, the bandwidth of the servo control system must hence be below this frequency. To raise this lowest resonance frequency one has to make a stiffer mechanism. Intuitively an increase in stiffness in the inner joint contributes the most to the lowest resonance frequency. A simulation showed that multiplying this stiffness by four raised the resonance frequency by 70%.

A more thorough dynamical analysis of the total mechanism and control systems is forming the basis for further research.

Acknowledgments

We wish to thank Fridtjov Irgens at the Norwegian Institute of Technology, Department of Mechanics, Thermo- and Fluid-Dynamics, for his contribution to the dynamic modelling. We also wish to thank Geir Moholdt and Ole Ivar Sivertsen at FEDEM A/S, N-7034 Trondheim, for their support with the FEDEM system.

References

Char, B. W., Geddes, K. O., Gonnet, G. H., Monagan, M. B. and Watt, S. M. (1988), MAPLE Reference Manual, University of Waterloo, Ontario, Canada.

Irgens, F. (1985a), *Statikk og Fasthetslære, Bind 1 og 2, 3.utgave* (Tapir Forlag).

Irgens, F. (1985b), *Dynamikk, 2.utgave* (Tapir Forlag).

Lien, T. K. (1992), Regneeksempel på motorsystem for håndteringsautomat, Lecture note, NTH 1992.

Opitz, H. (1970), *Moderne Produktionstechnik, Stand und Tendenzen* (W. Girardet, Essen).

Riven, E. I. (1988), *Mechanical Design of Robots*, Department of Mechanical Engineering, Wayne State University (McGraw-Hill).

Sintef Production Engineering (1993), FEDEM (Finite Element Dynamics in Elastic Mechanisms) Users Guide.